Electrophoretic NMR studies of polymer and surfactant systems

P. C. Griffiths, A. Paul and N. Hirst

Received 31st August 2005
First published as an Advance Article on the web 13th January 2006
DOI: 10.1039/b501286b

The aim of this *tutorial review* is to introduce to a broader readership the emerging technique of electrophoretic NMR (eNMR). The ''electrophoretic'' element of the technique refers to the fact that charged particles are induced to flow by the application of an electric field. This flow is measured using pulsed-gradient spin-echo NMR (PGSE-NMR). The great potential of this experimental approach is the fact that NMR is chemically selective and non-invasive. eNMR, especially when combined with the more established PGSE-NMR experiment, may therefore be used to quantify the structure of multi-component systems *via* the dynamics and charge of each species within a complex mixture. Accordingly, eNMR is likely to be of great significance for colloid scientists, biologists, technologists and formulation scientists.

1. Introduction

Surfactants—a concatenation of ''surface active agents''—are schizophrenic molecules; part of the molecule is hydrophobic, part is hydrophilic and the contrast between these characteristics leads to their many interesting and useful properties. Perhaps the most fundamental is the observation that at well defined concentrations, surfactants spontaneously self-assemble to form rather intricate structures, the simplest being the ''micelle''. This structure comprises the hydrophobic parts of the surfactant molecule forming a ''core'' largely shielded from the aqueous phase by the solvated polar headgroups. The polar headgroups may be nonionic or ionic (anionic or cationic), and the dissociation of the counterions associated with the ionic headgroups leads to the ionic character of the micelle.

School of Chemistry, Main Building, Park Place, Cardiff University, Cardiff, UK CF10 3AT

Peter Griffiths

Peter Griffiths graduated with a PhD from Bristol University in 1991, and after postdoctoral periods with Profs. Terence Cosgrove (Bristol University) and Peter Stilbs (Royal Institute of Technology, Stockholm), was appointed Lecturer at Cardiff in 1995, Senior Lecturer in 2001/2 and subsequently Reader in 2004. He serves on several committees whose role is to advance colloid and surface science within the UK. The research interests of his group focus on fundamental physico-chemical properties of ''soft matter''—structured fluid materials comprising particle, polymer and surfactants in a low molecular weight solvent—using several complimentary techniques ranging from spectroscopy to scattering.

Surfactants may also be characterised as an (association) ''colloid''. A colloid consists of ''dispersed'' microscopic particles (like the oil core of the micelle)—with a characteristic

Alison Paul

Alison Paul also graduated with a PhD in Colloid Science from Bristol University in 2001. After postdoctoral appointments in Bristol, Royal Institute of Technology (KTH), Stockholm, and the School of Chemistry Cardiff University, she is now based in the Welsh School of Pharmacy in Cardiff. Her current position is Senior Research Fellow and Project manager on an EPSRC funded ''Platform Grant'' on Bioresponsive Polymers. Her research interests lie in understanding the links between physico-chemical behaviour and therapeutic performance of polymeric drug delivery systems.

Natasha Hirst

Natasha Hirst graduated from Cardiff University in 2001 and is currently studying for a PhD in colloid science. Her research centres on the effects of solvency in polymer/surfactant systems.

length scale of the order of 1 nm to 1 μm—within a second "continuous" phase. Depending on the state of the dispersed and continuous phases, colloids encompass solid foams (gas in solid), emulsions (liquid in liquid) and smoke (solid in gas). Given this definition based on a characteristic dimension, polymer solutions may also be regarded as colloids; indeed, polymers and surfactants share many common properties.[1,2]

Electrophoresis is the transport of charged particles in an electric field; under the effect of a constant electric field E_{dc} ions of a particular species attain the steady-state velocity $v_e = \mu E_{dc}$, where μ is the electrophoretic mobility. The electrophoretic mobility is determined by the charge on a particular species and is of considerable interest in colloid chemistry because the (long range) Coulomb interaction is often the dominant interaction between colloidal structures.[3] From a non-colloid perspective, understanding the migration of ions in electric fields is also important as the separation of ions according to mobility criteria is the basis of several analytical techniques.[4]

1.1 Why electrophoretic NMR?

Electrophoresis is an established field, especially with respect to colloidal particles where it is possible to quantify their velocity using microscopy or laser Doppler approaches.[5] There are, however, few experimental techniques that measure the velocity of small molecules of interest (polymers or surfactant micelles) in complex, multi-component mixtures. This is due to the fact that the detection approach (light scattering, osmotic pressure, dielectric spectroscopy) cannot identify or distinguish between the various components. Essentially, a technique is required that is "chemically selective", and NMR is the most obvious candidate. In an electrophoretic NMR (eNMR) experiment (also known as DCNMR[6] or magnetic resonance electrophoresis MREP[7,8]), the electrophoresis element is analogous to standard electrophoresis methodology—an applied electric field generates a coherent motion in the sample, and the charged molecules acquire a velocity or flow dependent on their charge and size. This flow is quantified by encoding a spatial and temporal dependence to the NMR signal by the use of magnetic field gradients.[9,10] There are several approaches to quantifying the flow[11] and these are discussed later, but in one guise of the experiment, each chemically identifiable peak in the NMR spectrum will be modulated by the electrophoretic mobility of the species from which that peak originates. Adding the electrophoretic mobility dimension to the already well-established and highly versatile NMR stable of experimental techniques, is therefore likely to make a significant impact on colloid science (nanotechnology) and a range of biochemically related disciplines.

eNMR is however, not a particularly new technique. Proof of concept of eNMR was shown many years ago,[12] but the technique has undergone rapid development in recent years.[6,11,13–20] To set this review in context, eNMR prior to 1989 has been described in an excellent review by Johnson and He[18] with subsequent reviews by Holz[6] and Johnson.[11] This review builds heavily on those, focusing more on the data published in the last five years or so rather than the technique *per se*, although some technique relevant material is of course included. The reader might also find Callaghan's monograph[9] on NMR methods for the measurement of diffusion and flow of interest.

2. Theoretical aspects

2.1 Electrophoresis

Electrophoresis describes the motion of a charged colloidal particle due to the influence of an applied electric field, E_{dc}. Ultimately, the particle attains a constant drift velocity v_e when the electric force causing this motion balances the viscous drag or the resisting force due to the motion of the particle, a force that depends on the hydrodynamic radius (size and shape) of the particle and the viscosity of the medium. Frequently, the force is expressed in terms of a hydrodynamic potential such as the ζ-potential, corresponding to the charge of the colloid at the plane of shear, Fig. 1.

Quantifying the electrophoretic mobility μ of a species is a relatively straightforward task. However, general theories relating μ to molecular properties are complicated and often difficult to use. Counterions in an electrolyte solution (with viscosity η and relative dielectric constant ε_r) surrounding a particle (with radius a and charge Ze) screen the charge of that particle such that the effective potential drops to zero over a distance given by the inverse Debye screening length, κ^{-1}

$$\kappa = \sqrt{\left(\frac{2\rho F^2}{\varepsilon_o \varepsilon_r RT}\right) I_c} \tag{1}$$

where ρ is the density of the solvent, ε_o is the permittivity of vacuum, F is the Faraday constant, R is the gas constant, T is the absolute temperature, and I_c is the ionic strength. Making the assumption that the applied electric field does not distort the ionic atmosphere, Henry showed that the electrophoretic mobility is given by

$$\mu = \frac{Ze}{6\pi\eta a}\frac{X_1(\kappa a)}{(1+\kappa a)} \tag{2}$$

where $X_1(\kappa a)$ is a monotonically increasing function—the Henry function—that ranges from 2/3 for $\kappa a \ll 1$ to 1.0 for $\kappa a \gg 1$.

In the 'large particle' limit, where $\kappa a \gg 1$, eqn (2) is equivalent to $\mu = \sigma/\eta\kappa$, where σ is the surface charge density ($\sigma = Ze/4\pi a^2$). Smoluchowski showed that

$$\mu = \frac{\varepsilon_o \varepsilon_r \zeta}{\eta} \tag{3}$$

where ζ is the potential at the plane of shear (between the stationary and moving solvent layers). Thus, for $\kappa a \gg 1$, a measurement of the electrophoretic mobility provides a direct route to σ and to ζ. Note that there is no dependence of μ on particle size (a) or even particle shape. Accordingly, electrophoresis is a common technique for determining the surface charge on colloidal particles.[21]

In the 'small particle' limit where $\kappa a \ll 1$, eqn (2) may be recast into $\mu = Ze/f$, where $f = 6\pi\eta a$, by expressing the balance of electrostatic and frictional forces at steady state *i.e.*

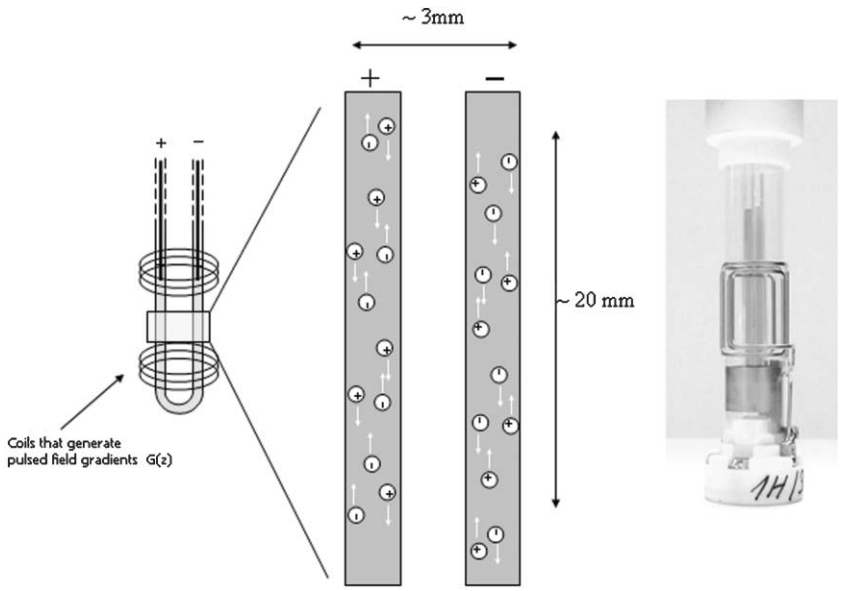

Fig. 1 Illustrative representation of the electrophoretic and diffusion components of the eNMR experiment. The photograph shows the location of the U-tube within the rf coil assembly, the schematic shows the location of the coils that generate the magnetic field gradient in the z (vertical) direction, whilst the enlargement in the middle shows the opposing direction of the flow of the ions within the two columns of the U-tube.

$ZeE_{dc} = fv_e$. Note now, there is a dependence of the electrophoretic mobility on size and shape *via f*.

$$\mu = \frac{Ze}{6\pi\eta a} \tag{4}$$

It is also common to find used an expression analogous to eqn (3);

$$\mu = \frac{2}{3}\frac{\varepsilon_0\varepsilon_r\zeta}{\eta} \tag{5}$$

Henry's equation can often be a crude approximation since the applied electric field may distort the ionic atmosphere. However, Henry's formula is accurate provided that the ζ-potential is small. Modern analytical treatments of this problem have been reviewed by Hunter.[21] A major difficulty with many if not all electrokinetic theories is that the results are expressed in terms of ζ-potentials, but the ζ-potential cannot be measured (except in the Smoluchowski limit) because the counterions inside the plane of shear move with the particle, thereby modifying the apparent surface charge density. Further, and of most significance here, surfactant and polymer containing systems rarely fall into one of these two limiting cases; for typical surfactant solutions ($r \sim 2$ nm and at ambient ionic strengths) $0.4 < \kappa r < 1$ and therefore, only approximate or relative values of the ζ-potential can be obtained.

2.2 Measuring electrophoresis by NMR

eNMR combines pulsed-gradient spin-echo NMR and *in situ* electrophoresis to directly determine the drift velocities of the NMR active ions in the electric field. A brief synopsis of the relevant theory is provided here but the reader is referred to other texts for a more detailed discussion.[9,22]

The drift velocities are quantified using a pair of field gradient pulses separated by a characteristic time *i.e.* PGSE-NMR. If a magnetic field gradient $g(z)$ is applied co-axially to the main magnetic field B_0, the effective magnetic field is $B_z = B_0 + g(z).z$. Viewing the spins within a frame of reference rotating with frequency $\omega_0 = -\gamma B_0$ about the z axis, application of the first of the two field gradient pulses of duration δ and amplitude $\gamma g(z)$, winds the spins into a helix with pitch $2\pi/\gamma\delta g(z)$. The second field gradient pulse, which is identical but of opposite phase to the first, unwinds this helix leading to a spin-echo. Diffusion of the molecules to a different position within the sample leads to a difference in the magnitude of the field gradient, which results in a loss of phase coherence and hence, spin-echo intensity.

If an electric field of duration t_1 is applied in the z-direction during the time interval between these two gradient pulses, the associated magnetisation helix is shifted in phase, $\theta = qv_et_1$ where v_e is the drift velocity. Therefore, the simplest method for measuring the presence of flow involves the determination of a phase shift.[11] However, if a U-tube electrophoretic cell has been used, the opposing direction of flow of the material in the two tubes (Fig. 1) renders the sign of the phase angle indeterminable. The magnitude of the phase angle is therefore determined by fitting the echo amplitude to a cosine function $\cos\left(\frac{q\mu It_1}{k_eA}\right)$ with current I as the experimental variable, knowing

$$E_{dc} = \frac{I}{k_eA} \tag{6}$$

where k_e is the conductivity and A is the cross-sectional area of the cell. Fig. 2 illustrates the sensitivity of this approach, presenting raw data for a series of mixed surfactant micelles where the charge is controlled by the micelle composition.

When the electrophoretic mobility is small, and/or in combination with a narrow range of accessible experimental variables, a more accurate method for determining the associated small phase change that results from the low drift velocity is to measure the phase shift of an off-resonance spin-echo, Fig. 3.[11] When the resonance offset $\Delta\omega_{or}$ is small such that $B_1 \gg \tau\Delta\omega_{or}$ and $\Delta\omega_{or} \gg 2/T_2^*$, the echo signal in the vicinity of 2τ is given by

$$S(t) \propto \cos(\Delta\omega_{or}t + \Delta\theta) \quad (7)$$

Under these conditions, $\Delta\theta = 0$ in the absence of the gradient pulses but is $\Delta\theta = qv_e t_1$ when the gradient pulses are present. Fig. 3 illustrates the shift t_s of the zero points when the field gradients are applied, from which $\Delta\omega_{or} = \pi/t_0$ and that $\Delta\theta = \pi t_s/t_0$. Although this method allows the drift velocity to be determined accurately when a single resonance line is present, it provides no information when more than one resonance line is present, and is therefore limited to rather simple systems.

By far the most productive experimental approach is to harness the data processing capability of the computer on the spectrometer; the (first) spin-echo in a 2D experiment is Fourier transformed, and the resultant spectrum is 'phased'. All subsequent spectra are phased with the same parameters and the peak associated with the ionic species of interest becomes modulated by the factor $\cos\left(\frac{q\mu I t_1}{k_e A}\right)$. The electrophoretic mobility of each species μ_i is then obtained from the period of the oscillation, Fig. 2.

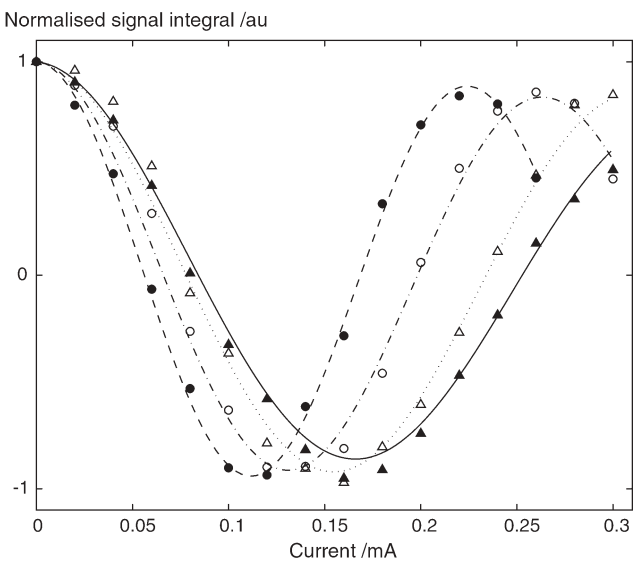

Fig. 2 Normalised signal intensity as a function of electric field current for a series of 50 mM surfactant solutions with $\alpha_{SDS} = 0.13$ (●), $\alpha_{SDS} = 0.37$ (○), $\alpha_{SDS} = 0.50$ (△) and $\alpha_{SDS} = 1.0$ (□). The data have been normalised following the procedure in the text. The lines through the data correspond to a fit to the cosine modulation. At this surfactant concentration, the solution mole fraction α_{SDS} = micelle mole fraction x_{SDS}. Reproduced with permission from *Langmuir*, 2001, **17**, 7178–7181.[52] Copyright 2001 American Chemical Society.

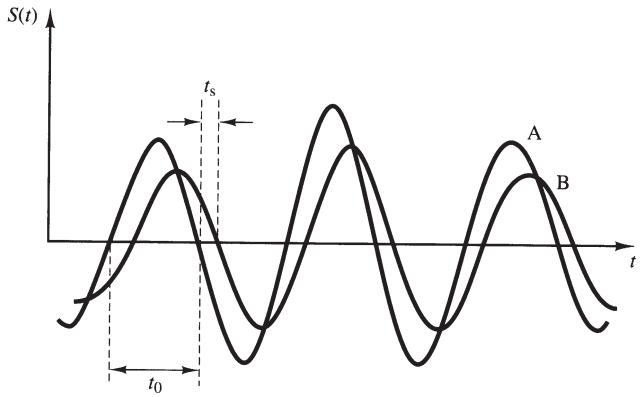

Fig. 3 Two off-resonance signals in the presence of flow (a) spin echo detected when the gradient is switched off (b) spin echo detected when the gradient is switched on. Reproduced with permission from *Electrophoretic NMR* by C. S. Johnson, in *Encyclopedia of Nuclear Magnetic Resonance*, ed. D. M. Grant and R. K. Harris.[11] Copyright 1996 Wiley and Sons Ltd.

3. Practical aspects

eNMR has come a long way since its conception, but in general, is far less straightforward than the NMR diffusion experiment it closely resembles since several non-electrophoresis artefacts complicate the measurement of the true electrophoretic mobility. Whilst these have all been recognised previously, these have only recently been investigated systematically by Stilbs *et al.*[23] To illustrate the current state of the art of eNMR, the salient features of that study are briefly discussed here.

3.1 Sample holder

Fig. 4 displays some of the common electrophoretic cell geometries that have been used to date. The U-tube (Fig. 4(a)) is the most common, but gives the counterflow of ions resulting in the loss of the signs of the mobilities. Furthermore, shimming with this configuration can be a problem. The cylindrical design (Fig. 4(b)) avoids these problems but is less convenient due to the required gel plug. The configuration shown in Fig. 4(c) has a better filling factor and the glass

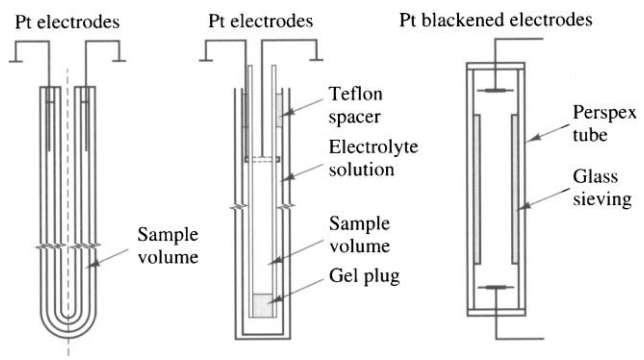

Fig. 4 Common sample environments. Reproduced with permission from *Electrophoretic NMR* by C. S. Johnson, in *Encyclopedia of Nuclear Magnetic Resonance*, ed. D. M. Grant and R. K. Harris.[11] Copyright 1996 Wiley and Sons Ltd.

sieving reduces electroosmosis, but any gas generated cannot escape. Platinum, blackened platinum, and Ag/AgCI electrodes have been used by various groups, with the latter two types decreasing gas production at the electrodes.

3.2 Sample heating

The electrophoretic current heats the sample during the time it is applied, and although heating in this fashion is homogeneous, cooling due to the tube walls leads to a parabolic temperature profile, and therefore convection. There are no practical solutions to his problem, except the use of convection compensated pulse sequences.

3.3 Electroosmosis

Electroosmosis is the biggest problem in eNMR and is often manifest as an apparent charge on a non-charged species such as water. Electroosmosis can occur in these systems caused by the build-up of an electric double-layer close to the charged glass surface due to the adsorbed counter-ions. This layer has a net charge and will therefore be subject to an electromotive force if an electric field is applied parallel to the wall. This results not only in the migration of the ions but also the flow of the liquid associated with them. Increasing the ionic strength decreases the double-layer thickness, and may offer a route to reducing electroosmosis, although for colloidal systems higher ionic strength often has a deleterious consequence for the sample. Whilst the true electrophoretic mobility may be obtained mathematically by a number of routes (subtracting the electroosmotic mobility for an uncharged probe species from the apparent mobility, or measuring the flow profile by flow imaging perpendicular to the branches of the U-tube and decoupling the electroosmotic and electrophoretic kinetics) by far the simplest solution is to suppress electroosmosis by coating the glass surface with a polymer such as poly(acrylamide) PAA.[24]

3.2 NMR pulse sequences

Many, if not all, of the problems discussed above can be alleviated by an electrophoretic version of the double stimulated echo pulse sequence, (EDSTE) Fig. 5.[23] The electrophoretic velocity field for ions changes sign on a nanosecond timescale when the electric field is switched, while other coherent displacements such as natural convection proceed unchanged. Hence, any constant velocity effects such as convection are filtered out while the electrophoretic phase modulation is maintained. There are other advantages to this pulse sequence, specifically (i) for a capillary geometry, electroosmotic flow builds up over $\sim$100 ms and is thereby suppressed by the faster polarity reversal and (ii) since the polarity is reversed, electrolysis is also reversed thereby suppressing the total volume of gas produced at the electrodes. Several of these aspects have been addressed experimentally by Manz *et al.*[25]

The optimised experiment configuration arrived at by Stilbs *et al.*[23] is a PAA-coated glass U-tube with two blackened Pt wires as electrodes immersed into the solution as depicted in Fig. 6, with this suspended in an NMR tube filled with D_2O,

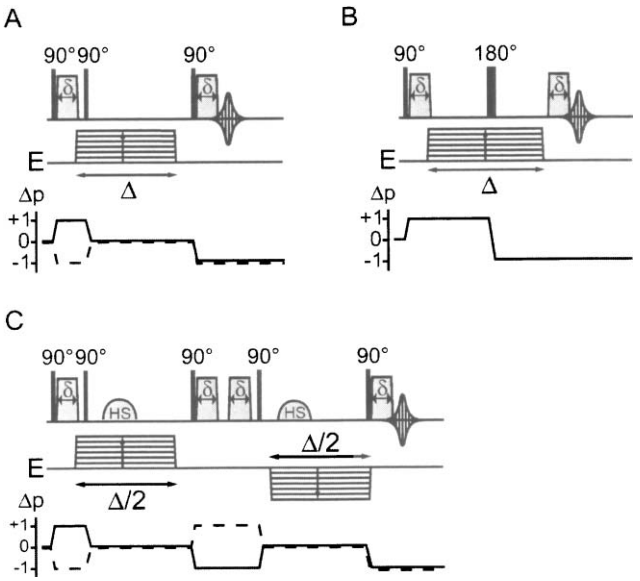

Fig. 5 Pulse sequences often used in electrophoretic NMR experiments; a) stimulated echo b) spin echo and c) double stimulated echo. Reproduced with permission from the Doctoral Thesis of Erik Pettersson, KTH, Stockholm, Sweden, 2005.

employing an EDSTE-based NMR sequence. This results in almost constant peak intensity for neutral molecules, while preserving the electrophoretic cosine modulation for ions. As may be seen in Fig. 7, the water signal decays by about 6% at the maximum current used, a figure that should be compared with an expected 5% decay due to the unavoidable Joule heating.

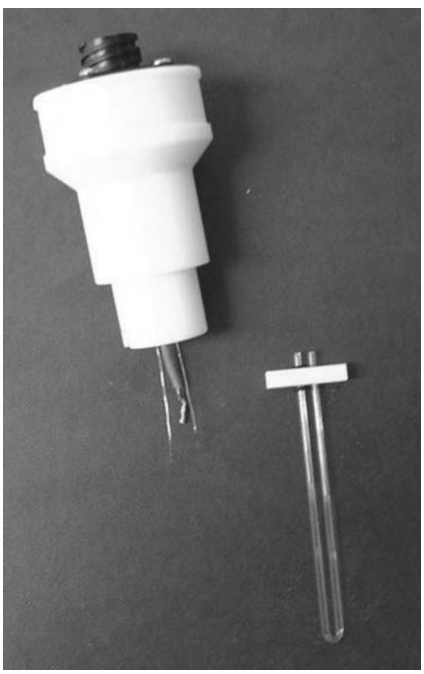

Fig. 6 Photograph of the U-tube electrophoretic cell developed by Stilbs *et al.* Copyright P. Stilbs.

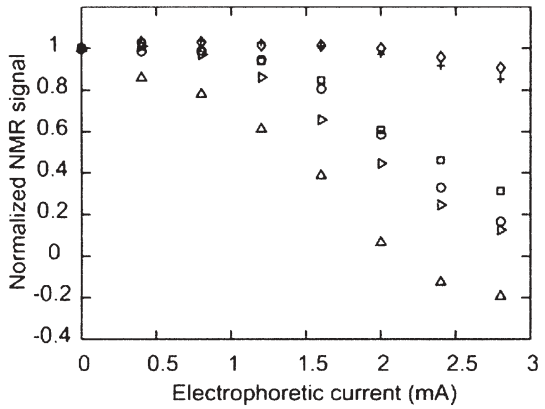

Fig. 7 The decay of integral intensity of the water peak for different experimental setups as function of the electrophoretic current. The electrophoretic experiment was performed with conventional stimulated echo detection (ESTE) (△) without polyacrylamide (PAA) coating on the tube walls; (▷) with tube walls coated by PAA; (○) with tube walls coated by PAA and with Pt-black cover on the electrodes; and (□) with tube walls coated by PAA, with Pt-black on the electrodes and with the U-tube immersed in perfluorinated oil. Experiments with double stimulated-echo detection (EDSTE) were also performed (+) with PAA coating and Pt-black on the electrode; and (◇) with PAA coating, Pt-black on the electrode and the U-tube immersed in D2O. Reproduced with permission from P. Stilbs *et al., Concepts in Magnetic Resonance*, 2004, **22**, 61.[23] Copyright 2004 Wiley and Sons Ltd.

4. Experimental investigations

The focus of this section is to give a comprehensive survey of recent data to illustrate the nature of the information available *via* eNMR. There have been some key papers that describe important applications of eNMR in a somewhat limited fashion (for example ion transport,[26–28] protein mixtures[29,30] and technique development[31,32]). These are outside the scope of this review and will not be further discussed. Rather, this review arbitrarily describes only those articles in which eNMR forms part of a larger experimental study, and it is intended that this will more fully demonstrate the capability and versatility of eNMR.

4.1 Polymeric systems

The presence of charged or ionisable groups on a polymer largely determines the behaviour of the polymer—solubility, tendency to adsorb at surfaces—and these may be controlled by changes in external variables such as pH or ionic strength. This character is harnessed in many diverse practical applications, such as waste water remediation, flocculation of fibres, ink fixing coatings in ink-jet paper and in drug delivery.[33]

4.1.1. Strong polyelectrolytes. eNMR has been applied to a number of strong polyelectrolytes by Scheler *et al.*[34–38] specifically a series of poly(acrylamide) copolymers (''Praestol''), (poly(styrene sulfonate) PSS and poly(diallyldimethylammonium chloride) PDADMAC. Fig. 8 reproduces typical raw experimental data for the eNMR experiment performed on PSS[37] whilst Fig. 9 illustrates the cosine fit to the intensities.

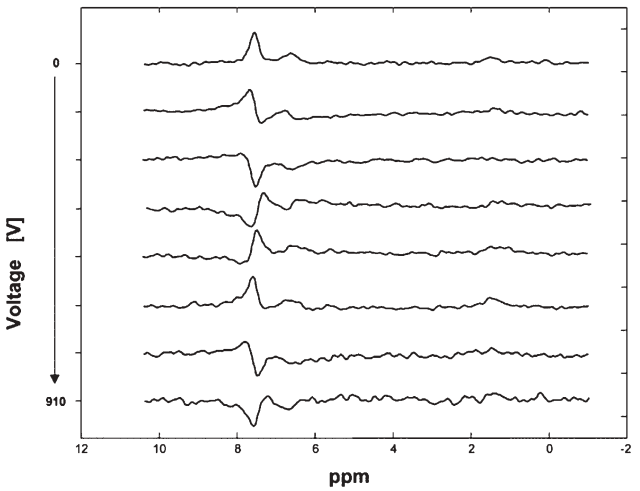

Fig. 8 Raw eNMR spectra for poly(styrene sulfonate) as a function of applied electric field. Reproduced with permission from U. Scheler *et al. Colloids and Surfaces, A*, 2003, **222**, 35.[36] Copyright 2003, Elsevier.

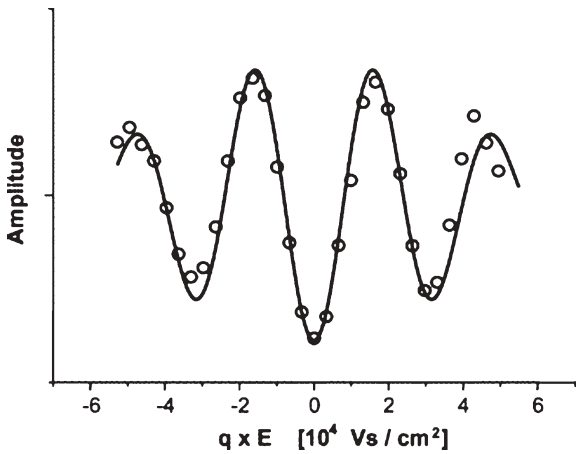

Fig. 9 Cosine fit to the intensities for poly(styrene sulfonate) PSS data presented in figure 8. Reproduced with permission from U. Scheler *et al. Colloids and Surfaces, A*, 2003, **222**, 35.[36] Copyright 2003, Elsevier.

In this series of papers, Scheler *et al.* showed that the charge on the polymer is accessible by setting the force due to the electrostatic nature of the polymer driving the flow equal to the frictional force opposing the flow;

$$ZeE_{dc} = \frac{k_b T}{D_s} v \tag{8}$$

where k_b is the Boltzmann constant and D_s is the self-diffusion coefficient. If the polymer self-diffusion coefficient is known

$$Z = \frac{k_b T \mu}{e D_s} \tag{9}$$

From this, Scheler *et al.* were able to compare and contrast the behaviour of the self-diffusion coefficient, the fractal dimension and electrophoretic mobility as a function of ionic strength. For the PSS,[36,37] (M_w = 77,000 g mol^{-1}), the

self-diffusion coefficient and fractal dimension increased whilst the electrophoretic mobility initially increased but ultimately dropped with increasing ionic strength. Taken together, these results showed that the effective charge on the PSS decreased from $\sim$37 to 20 over the salt range $0 < [NaCl] < 0.04$ mol l^{-1}, as a reflection of the increased condensation of the counterions onto the polymer. Similarly, the same authors showed that the charge on the Praestol copolymer scaled linearly with ionic composition.[35]

4.1.2 Weak polyelectrolyte. Poly(ethylene imine) PEI in aqueous solution is largely uncharged at high pH, but at low pH exhibits one of the highest charge densities of any polyelectrolyte.[39] Its branched globular architecture results in very little coil expansion[40,41] over the pH range $2 < pH < 11$, *i.e.* the range over which the fractional charge on the polymer varies from 1 to 0. Therefore, branched PEI is a suitable choice to probe the molecular weight dependence of the electrophoretic mobility of the polymer as a function of pH, without the complicating factors of significant pH induced changes in conformation and self-diffusion coefficient as observed in the PSS and Praestol work.

The self-diffusion coefficient and electrophoretic mobility of two molecular weights of PEI (M_w = 2,000 g mol^{-1} and 25,000 g mol^{-1}) were recorded over a wide range of pH, $4 < pH < 13$. There was little change in the self-diffusion coefficient for each polymer over this pH range, but there was a pronounced molecular weight dependence, consistent with the expected change in size. The electrophoretic NMR data are presented in Fig. 10.[42] As can be seen, the electrophoretic mobility shows no dependence on molecular weight, but a significant step-change is observed around the pK_a of the PEI (pK_a = $\sim$10). The consistency of results between the different molecular weights may be rationalised by noting that the charge on the polymer scales linearly with the number of ionisable groups, and therefore to a first approximation, molecular weight *i.e.*

$$Z(\mathrm{pH}) = \alpha(\mathrm{pH})\frac{M_w}{RMM} \qquad (10)$$

where α(pH) is the pH dependent fractional charge on the polymer and RMM is the molar mass of the monomer unit. The self-diffusion coefficient scaled linearly with molecular weight $D_s \propto M_w^{-1}$ and since $z \propto M_w^{+1}$ (eqn (10)), the electrophoretic mobility, being proportional to the product $z\,D_s$ (eqn (9)), scales as M_w^0 *i.e.* is independent of molecular weight, as shown in Fig. 10.

In Fig. 11, the fractional charge on the polymer calculated from the pH titration is compared with the normalised fractional charge calculated from the electrophoretic NMR results. Clearly, there is a significant difference between the magnitudes of the degree of protonation extracted from the two approaches. One possible reason for this could be the effects of ionic strength as shown by Scheler *et al.* However, if one uses Manning's model of counterion condensation[43] to calculate an electrophoretic friction factor, strictly only valid for linear polymers and thence the fractional charge on the polymer, the electrophoretic mobility measurements are further reduced by a factor of approximately 2–3 and the agreement between the two approaches improves. Nonetheless, further work is required to consolidate the contribution that eNMR may make to this area.

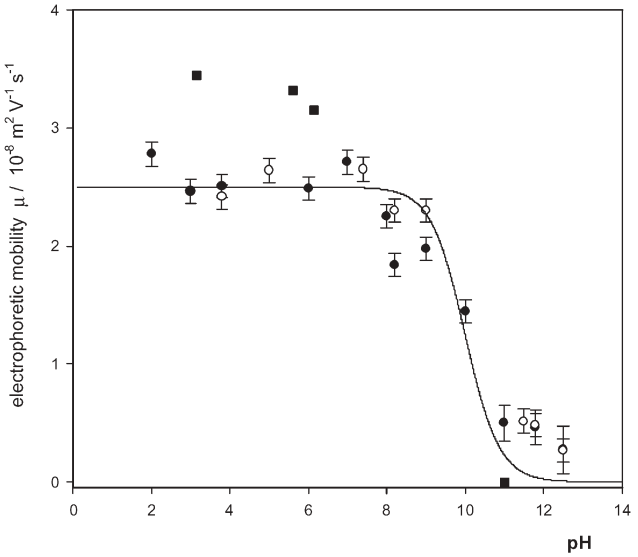

Fig. 10 The electrophoretic mobility of two samples of branched poly(ethylene imine) PEI as a function of pH; closed symbols M_w = 2,000 g mol^{-1} open symbols M_w = 25,000 g mol^{-1}. Shown for comparison is the predicted charge (line) based on p$K_a \sim 10$. The solid squares are data for PEI of M_w = 7,200 g mol^{-1} in 0.1 N NaCl (G. H. Lindquist and R. A. Stratton, *J. Coll. Int. Sci.*, 1976, **55**, 45.[71]) Reproduced with permission from P. C. Griffiths *et al.*, *Macromolecules*, 2005, **38**(8), 3539–3542.[42] Copyright 2005 American Chemical Society.

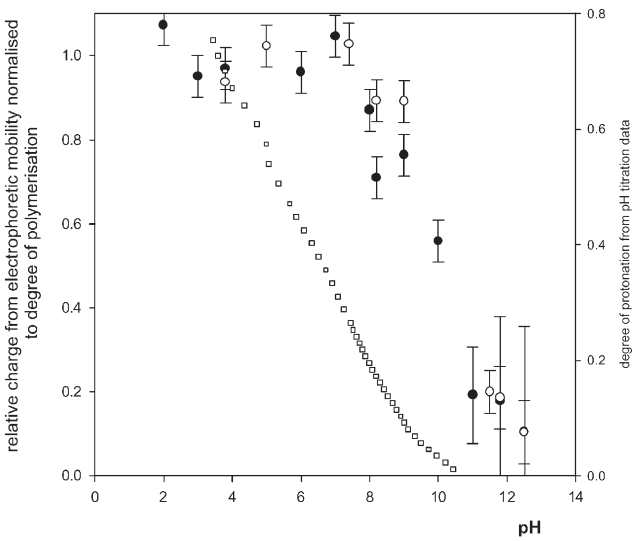

Fig. 11 The charge from electrophoretic mobility measurements for the two samples of branched PEI in Fig. 10, M_w = 2,000 g mol^{-1} (closed symbols) and M_w = 25,000 g mol^{-1} (open symbols) as a function of pH (left hand axis). The open squares are the comparable parameter calculated from M_w = 2,000 g mol^{-1} pH titration data (right hand axis). Reproduced with permission from P. C. Griffiths *et al., Macromolecules*, 2005, **38**(8), 3539–3542.[42] Copyright 2005 American Chemical Society.

4.2 Surfactant systems

4.2.1 Single surfactant solutions: surfactants with macrocounterions[44]. One of the more challenging parameters to model in terms of surfactant micellisation, is the degree of counterion dissociation α, and whether α determines or is a consequence of the size and shape of the surfactant micelle. Since the charge of an ionic micelle arises from the distribution of counterions according to electrostatic interactions between headgroups and counterions at the micelle surface, a combination of PGSE-NMR and eNMR is an ideal combination to probe the degree of counterion dissociation.

Recently, Bales *et al.*[45] have proposed the thesis that the micelle aggregation number N is a simple reflection of the aqueous phase concentration of counterions C_{aq},

$$N = N(C_{aq}) \quad (11)$$

C_{aq} is calculated according to eqn (12), and embodies surfactant solutions in which the "counterions" arise from monomeric surfactant, counterions dissociated from the micelle surface and any added salt

$$C_{aq} = F((\alpha([\text{surfactant}] - [\text{monomer}]) + [\text{monomer}] + C_{ad}) \quad (12)$$

where $F = 1/(1 - \phi)$, the correction factor for the micelle excluded volume and the square brackets denote concentrations. Hence, it is possible to prepare a series of solutions of surfactant and salt such that the overall free counterion concentration C_{aq} and therefore aggregation number N, is invariant across a wide range of surfactant concentration—a so called "constant C_{aq} series".[45] A recent study of sodium dodecyl sulfate (SDS), dodecyl trimethyl ammonium chloride (DTAC) and bromide (DTAB) using small-angle neutron scattering (SANS) coupled with time resolved fluorescence quenching (TRFQ) showed this to be a valid approach,[46] a concept subsequently generalised by Bales *et al.*[47–50]

These are particularly interesting systems for eNMR (and PGSE-NMR) since if by a suitable choice of system, both the surfactant and the counterion bear protons that exhibit peaks at quite different chemical shifts, it is possible to study their individual mobilities (diffusion and electrophoretic mobility) in this complex mixture. The tetramethyl ammonium dodecylsulfate (TMADS) system is one such example.[44] Due to the large difference in effective size between monomeric *versus* micellised surfactant, and associated/dissociated counterions, and taking into account the different charges on each species, the diffusion coefficient and electrophoretic mobility of each species will be quite different, and each will vary depending on the effects of sample composition on the equilibrium between micellised and non-micellised states Fig. 12. For example, the diffusion decay of the methylene resonance associated with dodecyl group reflects the concentration-weighted average mobility of monomeric and micellised surfactant;

$$<M_{(\text{measured})}> = M_{(\text{micelle})}(1 - x_{(\text{monomer})}) + x_{(\text{monomer})}M_{(\text{monomer})} \quad (13)$$

where M is the mobility parameter (electrophoretic mobility μ or self-diffusion coefficient D_s) and $x_{monomer}$ is a monomer

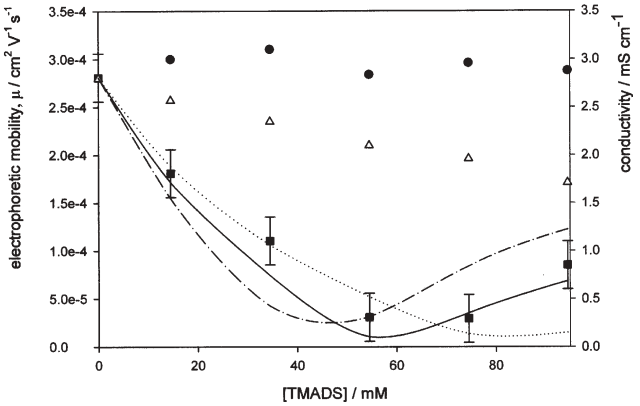

Fig. 12 eNMR and conductivity data for TMADS constant C_{aq} series [TMA^+] = 39.9 mM. Cosine fit to equation TMA^+ ions (filled squares) and micelles (filled circles). Also shown are conductivity data (open triangles). Lines are predictions based on various values of α; 0.25 (dash-dot), 0.35 (solid), 0.45 (dotted). Reproduced with permission from A. Paul *et al. J. Phys. Chem.*, 2005, **109**, 15775.[44] Copyright 2005 American Chemical Society.

mole fraction, whereas the behaviour of the methyl resonance arising from the TMA^+ ion reflects contributions from both bound and free counterions;

$$<M_{(TMA)^+}> = x_{(TMA)^+}M_{(TMACl)} + (1 - x_{(TMA)^+})M_{(micelle)} \quad (14)$$

where $x_{(TMA)}$ is the mole fraction of TMA^+ counterions in solution, including contributions from monomeric surfactant and those dissociated from the micelles,

$$x_{TMA^+} = \frac{[\text{monomer}] + \alpha([\text{surfactant}] - [\text{monomer}])}{[\text{surfactant}]} \quad (15)$$

Hence, from a simultaneous fit to eNMR and PGSE-NMR data Fig. 12, it is possible to calculate α. The degree of counterion dissociation for TMADS/TMACl is found to be constant within experimental error $\alpha_{TMA^+} = 0.34 \pm 0.05$ throughout the C_{aq} series. This combination of NMR techniques is potentially more informative than other more commonly employed (but simpler) techniques (*e.g.* conductivity) due to the chemical specificity of NMR.

4.2.2 Binary surfactant solutions: sodium dodecylsulfate (SDS)–dodecyl malono-bis *N*-methylglucamide (C_{12}BNMG) mixtures[51,52] and SDS–tetra(ethylene oxide) dodecyl ether (C_{12} E_4) mixtures[53]. Mixtures of surfactants are used widely in industrial and domestic formulations.[1,2] Whilst each component has a particular function (*e.g.* surface tension lowering, wetting, active ingredient deposition and control of stability or rheology), the properties of the complex mixture is invariably different to those of the individual components. Understanding the interactions between the various components is therefore crucial to optimizing their performance, and the degree of counterion dissociation is again a key parameter.[54]

As has been shown, the electrophoretic mobility is a useful parameter with which to explore α, and has been measured for a series of mixtures of SDS and the nonionic sugar surfactant

dodecyl malono-bis *N*-methylglucamide (C_{12}BNMG), as a function of micelle composition, x_{SDS}. This is a particularly interesting system as there is no change in aggregation number with composition, thus permitting α to be studied in isolation to any changes in micelle size and shape.

Representative data for such mixed micelles are shown in Fig. 13.[51,52] (Incidentally, the raw data are presented in Fig. 2.) The ζ-potential for these mixed micelles can be estimated from the micellar mobility by adopting the large-particle limit approach (eqn (3)). As the relationship between ζ-potential and mobility is linear, both values are given in the figure. Over the mole fraction range $0.2 < x_{SDS} < 0.8$, these ζ-potentials are greater than a simple linear interpolation between the two limiting compositions, indicating that a significantly higher fraction of the sodium ions must be dissociated from the micelle surface compared with the case of simple SDS micelles. At higher SDS mole fractions, the ζ-potential tends towards the linear interpolation between the two limiting cases, indicating that the sodium counterion dissociation must tend towards the simple SDS case as the surface becomes more SDS-like. The re-adsorption of sodium ions reduces the electrostatic repulsion between the headgroups in order that they can attain the separation required by the volume of the hydrophobic tail.

A parallel study was also performed on systems comprising SDS and the non-ionic surfactant tetra(ethylene oxide) dodecyl ether ($C_{12}E_4$).[53] The main distinction between these two systems is that in the SDS–C_{12}BNMG system, micelle size and shape is invariant with composition whereas addition of $C_{12}E_4$ to SDS micelles leads to significant micelle growth. For SDS–$C_{12}E_4$, with increasing non-ionic content, the aggregation number increases and the micelle becomes more elliptical.

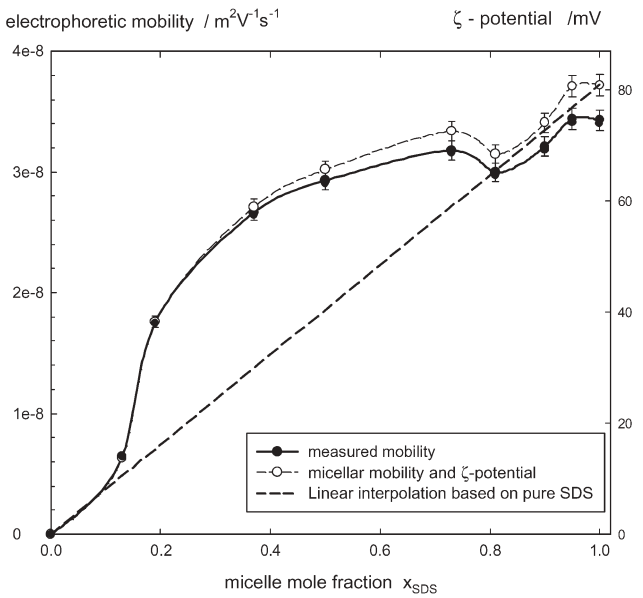

Fig. 13 Measured (•) and corrected (○) electrophoretic mobilities (left hand scale) as a function of SDS mole fraction x_{SDS} for 50 mM surfactant solutions. The corresponding ζ-potentials are shown on the right hand scale. Reproduced with permission from P. C. Griffiths *et al.*, *Langmuir*, 2001, **17**, 7178–7181.[52] Copyright 2001 American Chemical Society.

Associated with this shape change is a reduction in hydration of the surfactant headgroups. The degree of sodium counterion dissociation and ζ-potential shows an initial small decrease with decreasing SDS micelle mole fraction but subsequently increases, Fig. 14, reflecting the interplay between the electrostatic character of the micelle surface and the micelle curvature.

It is interesting to compare these two systems; the electrophoretic mobility of the mixed anionic–non-ionic surfactant system comprising SDS–$C_{12}E_4$ system *increases*—albeit after an initial drop—with increasing nonionic composition, whereas the SDS–C_{12}BNMG *decreases*. Thus, changes in the electrophoretic mobility may arise due to changes in both micelle size/shape *and* counterion binding. An approach to deconvolute these various effects has been advanced.[53] The effective charge on the micelle, $e_{effective}$, arises due to counterion dissociation characterised by $\alpha_{Na+}^{mixedmicelle}$. The behaviour of $\alpha_{Na+}^{mixedmicelle}$ *versus* micelle composition, x_{SDS} for these two systems is shown in Fig. 15.

It was concluded that as SDS molecules present in the micelle are replaced by $C_{12}E_m$, there is no significant change in the overall degree of sodium counterion binding. For other poly(ethoxylated) surfactants with a greater number of ethylene oxide units,[55–57] and for dimethyl phosphine and dimethyl amine,[58] this is not the case and a decrease in counterion binding is generally observed due to the decreasing surface charge density as the headgroup of the ionic surfactant is diluted over the micelle surface. For short chain ethoxylated surfactants and the SDS–C_{12}BNMG surfactants, no significant change is observed in the counterion binding, at least over the composition range that is rich in ionic surfactant, $x_{SDS} > 0.8$, in agreement with the theoretical predictions of Hall *et al*[59] and Maeda *et al.*[60]

4.2.3 Microemulsion based systems. Surprisingly, there have been few microemulsion studies performed by eNMR. One

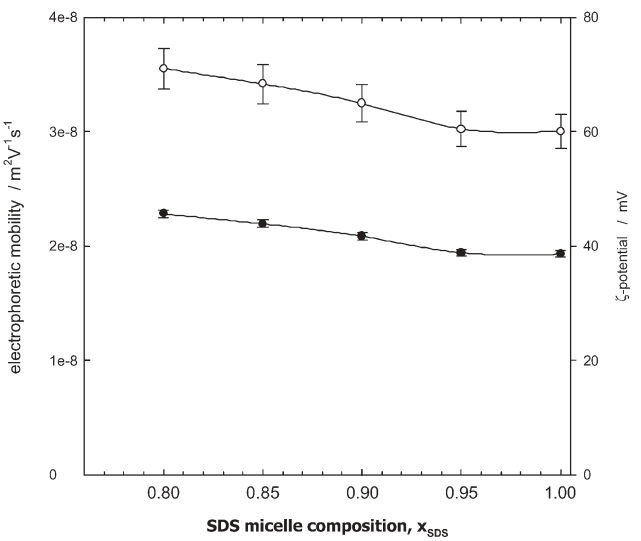

Fig. 14 ζ-Potential (•) calculated from the large particle limit for mixed micelles calculated from the electrophoretic mobility (O) for mixed micelles comprising sodium dodecylsulfate SDS and $C_{12}E_4$ as a function of micelle composition x_{SDS}.

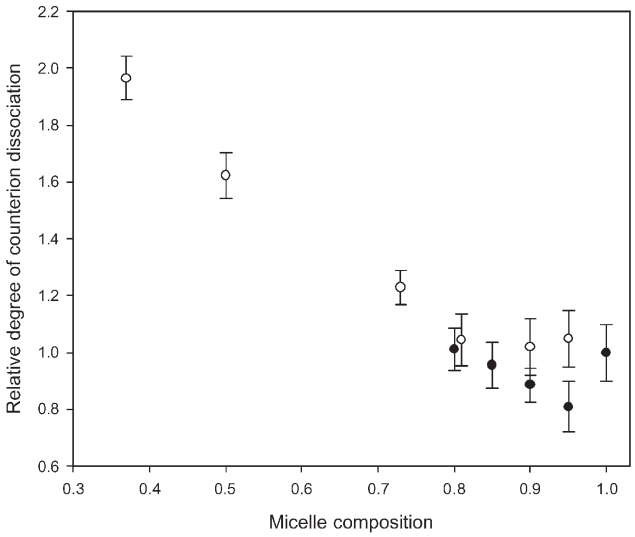

Fig. 15 Relative degree of counterion dissociation

$$\frac{\alpha_{\text{counter-ion}}^{\text{binary mixture}}}{\alpha_{\text{counter-ion}}^{\text{pure single compnent}}}$$

as a function of micelle composition (expressed in terms of the ionic surfactant mole fraction) for SDS–dodecyl malono-bis-*N*-methyl-glucamide (C_{12}BNMG) (open circles) and SDS–tetra(ethylene oxide) dodecyl ether ($C_{12}E_4$) (filled circles) calculated from the large particle limit formulism.

such[11] considered a sample prepared with triisopropylbenzene (TIPB) as oil phase, with $CH_3(CH_2)_{11}(OCH_2CH_2)_4OH$ (Brij 30) and sodium dodecyl sulfate (SDS) as the surfactants. The peak height *versus* current plots shown in Fig. 16 can be fitted to cosine functions to obtain the mobilities. The mobilities for TIPB and the surfactant peaks were identical, indicating that these components move together in the microemulsion droplets.

4.3 Polymer–surfactant systems

4.3.1 Surfactant–polymer mixtures. Mixtures of water-soluble polymers and surfactants have numerous applications in industry. Non-ionic polymers and anionic surfactants[61] show strong interactions due to the adsorption of polymer segments into the micelle palisade layer,[62] shielding part of the hydrophobic core of the micelle from the aqueous phase.

Stilbs *et al.*[63] measured the self-diffusion and electrophoretic mobility within a system comprising poly(ethylene oxide) and the anionic surfactant SDS. Changes in the self-diffusion of the species, often associated with the onset of an interaction between these two components, were correlated with changes in the electrophoretic mobility, Fig. 17. The electrophoretic mobility of the (non-ionic) polymer was essentially constant until the concentration at which the interaction starts, above which the mobility increases as the charged surfactant is added to the solution. This combination of techniques was shown to yield the correct charge for the surfactant anion 1.08 $\pm$ 0.04, and an estimate for the charge on an SDS micelle, 35.4 $\pm$ 1.8. From these data, the authors calculate ζ = 100 mV, in good agreement with a numerical solution of the Poisson–Boltzmann equation for a micelle. Again, this study illustrates the complementarity of eNMR and PGSE-NMR, and separates effects due to changes in conformation (diffusion) and charge (eNMR) associated with surfactant micelle binding.

4.3.2 The effects of solvency on surfactant micellisation and polymer/surfactant complexation. In many applications, surfactants are formulated with a variety of additives to achieve a desired range of properties and alcohols are frequently used as a cosurfactant. With increasing concentration of alcohol, the solubility of an ionic surfactant increases, the dielectric constant of the solvent decreases,[64,65] but the surface charge density in the palisade layer becomes more diluted. Short chain alcohols generally act as co-solvents,[66,67] medium chain alcohols partition between the palisade region and the aqueous solution[68] whereas long chain alcohols are solubilised into the micellar core. Therefore, there is a coupling between the charge on the micelle and its impact on the micellisation and the solvent composition. Polymers are also often present in formulations, and the interactions between surfactant and polymer (*e.g.* binding of surfactant monomers and micelles to the polymer chain) may also respond to changing solvent composition.[69]

Fig. 18 shows some preliminary data[70] to illustrate the interplay between the tendency of the micelle to bind to a

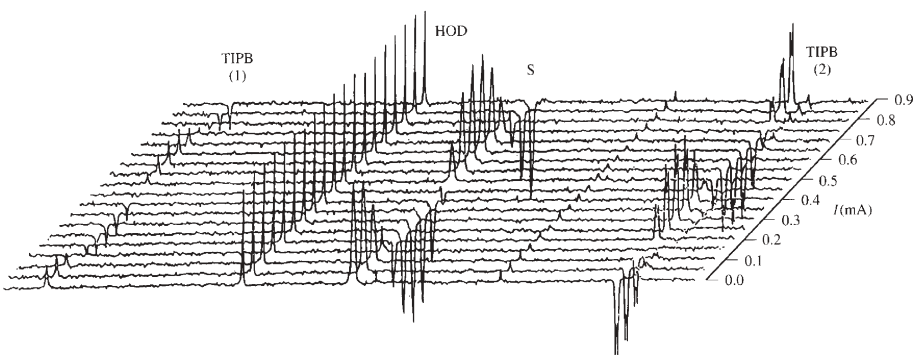

Fig. 16 Microemulsion eNMR data showing the identical cosine modulation for the surfactant and oil peaks and the constant intensity for the water peak. Reproduced with permission from *Electrophoretic NMR* by C. S. Johnson, in *Encyclopedia of Nuclear Magnetic Resonance*, ed. D. M. Grant and R. K. Harris.[11] Copyright 1996 Wiley and Sons Ltd.

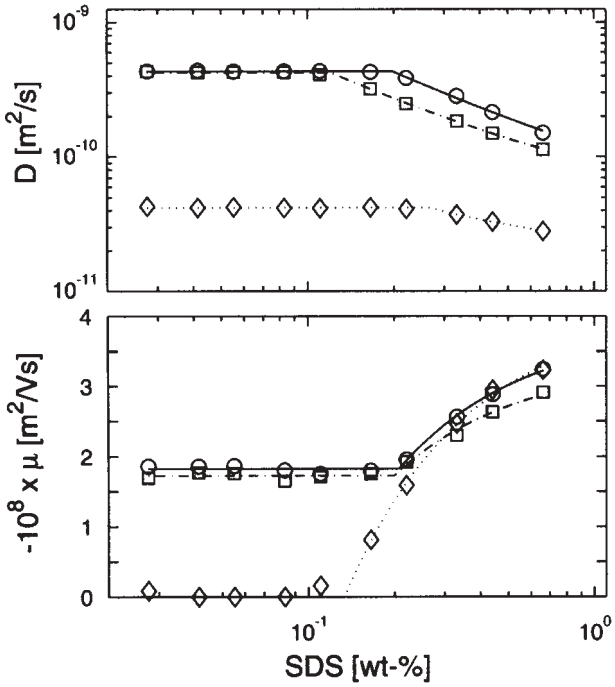

Fig. 17 Behaviour of the self-diffusion coefficient (upper panel) and electrophoretic mobility (lower panel) for SDS in the absence (open circles) and presence (open squares) of PEO and the PEO itself (open diamonds). Reproduced with permission from P. Stilbs *et al.*, *Langmuir*, 2004, **20**, 1138.[63] Copyright 2004 American Chemical Society.

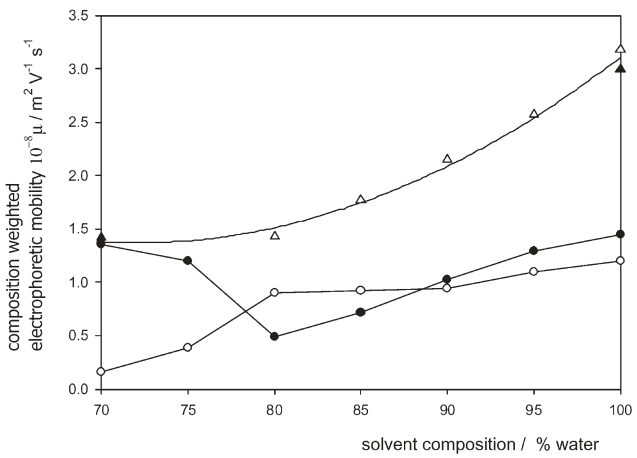

Fig. 18 Electrophoretic mobility in aqueous/ethanol solutions for (i) 30 mM SDS (open triangles) and one repeat measurement (closed triangles); (ii) 70 mM SDS in the presence of 5wt% PVP–SDS peak (closed circles) and PVP peak (open circles).

polymer, the charge on the polymer–surfactant complex, and the counterion dissociation.

In the absence of any added polymer, the electrophoretic mobility of SDS decreases with increasing ethanol content, due to the reducing charge on the micelle commensurate with a drop in aggregation number. The degree of counterion dissociation is largely invariant with solvent composition. On addition of the non-ionic polymer, poly(vinyl pyrrolidone) PVP (M_w = 40,000 g mol^{-1}), and for pure aqueous solutions, there is strong polymer surfactant complexation and the electrophoretic mobility of the SDS is greatly reduced compared to the no-polymer case, and the polymer has acquired some electrophoretic mobility due to the bound anionic micelles. On addition of ethanol, the tendency for the polymer and surfactant to interact is reduced, and accordingly the electrophoretic mobility of both the polymer and surfactant decrease. The drop in the SDS case is far more pronounced than that for the PVP, and indeed the two curves appear to cross, reflecting the contribution from the monomeric surfactant. For ethanol contents greater than 20%, the electrophoretic mobility of the polymer drops precipitously towards zero and that of the SDS tends towards the no-polymer behaviour, both reflecting that the interaction between the PVP and SDS ceases at 25% ethanol. This insight is not easily gained by common surfactant science methodologies such as surface tension and fluorescence due to the complicating factors of changes induced by the solvent composition.

5. Future outlook

eNMR is proving to be a highly versatile technique, in particular for the study of charge effects in polymer and surfactant containing systems. The strength of eNMR builds on the unique features of NMR, namely chemical specificity and non-invasiveness. In this regard, eNMR is highly complementary with its more established cousin, PGSE-NMR, and together, these approaches represent very significant tools for the chemist. eNMR is not without its drawbacks, in particular the insensitivity of NMR and the rather intricate control one must impose on the sample environment, but these issues are being addressed and significant progress has been made. Given the fact that most of today's NMR spectrometers are equipped with field gradient capability, the additional requirements for the electric field components are minor; over the next 5 years or so (the time period of the material in this review), eNMR will continue to flourish.

References

1 K. Holmberg, B. Jönsson, B. Kronberg and B. Lindman, *Surfactants and Polymers in Aqueous Solution*, 2nd edn., Wiley, Chichester, England, 2002.
2 D. Fennell Evans and H. Wennerström, *The Colloidal Domain; Where Physics, Chemistry, Biology and Technology Meet*, 2nd edn., Wiley-VCH, Weinheim, 1999.
3 J. N. Israelachvili, *Intermolecular and Surface Forces*, 2nd edn., Academic Press, London, 1992.
4 R. Westermeier, *Electrophoresis in Practice*, 3rd edn., Wiley-VCH, Weinheim, 2001.
5 J. Callejas-Fernández, M. Tirado-Miranda, M. Quesanda-Pérez, G. Odriozola-Prego and A. Schmitt, *Encyclopedia of Surface and Colloid Science*, vol. 3, ed. A. T. Hubbard, Marcel Dekker, New York, 2002, p. 4072.
6 M. Holz, *Chem. Soc. Rev.*, 1994, **23**, 165.
7 F. M. Coveney, J. H. Strange, A. L. Smith and E. G. Smith, *Colloids Surf.*, 1989, **36**, 193.
8 F. M. Coveney, J. H. Strange and E. G. Smith, *Mol. Phys.*, 1992, **75**, 127.
9 P. T. Callaghan, *Principles of Nuclear Magnetic Resonance Microscopy*, OUP, Oxford, 1991.
10 W. S. Price, *Concepts Magn. Reson.*, 1997, **9**, 299.

11 C. S. Johnson, 'Electrophoretic NMR', in *Encyclopedia of Nuclear Magnetic Resonance*, ed. D. M. Grant and R. K. Harris, Wiley & Sons, Chichester, England, 1996, p. 1886.
12 K. J. Packer, *Mol. Phys.*, 1969, **17**, 355–368.
13 M. Holz and C. Müller, *Ber. Bunsen-Ges. Phys. Chem.*, 1982, **86**, 141.
14 T. R. Saarinen and C. S. Johnson, *J. Am. Chem. Soc.*, 1988, **110**, 3332.
15 Q. H. He and C. S. Johnson, *J. Magn. Reson.*, 1989, **85**, 181.
16 T. R. Saarinen and C. S. Johnson, *J. Am. Chem. Soc.*, 1988, **110**, 3332.
17 M. Holz, O. Lucas and C. J. Müller, *Magn. Reson.*, 1984, **58**, 294.
18 C. S. Johnson and Q. He, Electrophoretic NMR in *Advances in Magnetic Resonance*, ed. W. S. Warren, Academic Press, San Diego, 1989, p. 133.
19 Q. H. He, Y. M. Liu, H. H. Sun and E. C. Li, *J. Magn. Reson.*, 1999, **141**, 355.
20 Q. H. He, W. Lin, Y. M. Liu and E. C. Li, *J. Magn. Reson.*, 2000, **147**, 361.
21 R. J. Hunter, *Foundations of Colloid Science*, OUP, Oxford, Vol. 1, 1987, Vol 2, 1989.
22 O. Söderman and P. Stilbs, *Prog. Nucl. Magn. Reson. Spectrosc.*, 1994, **25**, 445.
23 E. Pettersson, I. Furó and P. Stilbs, *Concepts Magn. Reson.*, 2004, **22**, 61.
24 S. Hjertén, *J. Chromatogr.*, 1985, **347**, 191.
25 B. Manz, P. Stilbs, B. Jönsson, O. Söderman and P. T. Callaghan, *J. Phys. Chem.*, 1995, **99**, 11297.
26 H. J. Walls, P. S. Fedkiw, T. A. Zawodzinski and S. A. Khan, *J. Electrochem. Soc.*, 2003, **150**, 165.
27 M. Holz, S. R. Heil and I. A. Schwab, *Magn. Reson. Imaging*, 2001, **19**, 457.
28 M. Ise, K. D. Kreuer and J. Maier, *Solid State Ionics*, 1999, **125**, 213.
29 Q. He, Y. Liu and T. Nixon, *J. Am. Chem. Soc.*, 1998, **120**, 1341.
30 Q. He, W. Lin, Y. Liu and E. Li, *J. Magn. Reson.*, 2000, **147**, 361.
31 S. R. Heil and M. Holz, *Angew. Chem., Int. Ed. Engl.*, 1996, **35**, 1717.
32 M. Holz, D. Seiferling and X. Mao, *J. Magn. Reson., Ser. A*, 1993, **105**, 90.
33 P. C. Griffiths, A. Paul, Z. Khayat, K.-W. Wan, S. M. King, I. Grillo, R. Schweins, P. Ferruti, J. Franchini and R. Duncan, *Biomacromolecules*, 2004, **5**, 1422.
34 U. Böhme and U. Scheler, *Macromolecular Symposium*, 2004, **211**, 87.
35 S. Wong and U. Scheler, *Colloids Surf., A*, 2001, **195**, 253.
36 U. Böhme and U. Scheler, *Colloids Surf., A*, 2003, **222**, 35.
37 U. Böhme and U. Scheler, *Polym. Prepr. (Am. Chem. Soc., Div. Polym. Chem.)*, 2003, **44**, 353.
38 U. Böhme and U. Scheler, *Macromol. Symp.*, 2002, **184**, 349.
39 G. E. Ham, in *Polymeric Amines and Ammonium Salts*, ed. E. J. Gothals, Pergamon Press, Oxford, 1980.
40 S. Kobayashi, K. Hiroshi, M. Tokunoh and T. Saegusa, *Macromolecules*, 1987, **20**, 1496.
41 P. C. Griffiths, Unpublished Results.
42 P. C. Griffiths, A. Paul, E. Pettersson and P. Stilbs, *Macromolecules*, 2005, **38**, 3539.
43 G. S. Manning, *J. Phys. Chem.*, 1981, **85**, 1506.
44 A. Paul, P. C. Griffiths, P. Stilbs, E. Pettersson, R. Zana and B. L. Bales, *J. Phys. Chem. B*, 2005, **109**, 15775.
45 B. L. Bales, *J. Phys. Chem. B*, 2001, **105**, 6798.
46 P. C. Griffiths, A. Paul, R. K. Heenan, J. Penfold, R. Ranganathan and B. L. Bales, *J. Phys. Chem. B*, 2004, **108**, 3810.
47 M. Benrraou, B. L. Bales and R. Zana, *J. Phys. Chem. B*, 2003, **107**, 13432.
48 B. L. Bales, K. Tiguida and R. Zana, *J. Phys. Chem. B*, 2003, **108**, 13948.
49 R. Zana, M. Benrraou and B. L. Bales, *J. Phys. Chem. B*, 2004, **108**, 18195.
50 B. L. Bales and R. Zana, *Langmuir*, 2004, **20**, 1579.
51 P. C. Griffiths, A. Paul, P. Stilbs and E. Pettersson, *Langmuir*, 2003, **19**, 8605.
52 P. C. Griffiths, E. Pettersson, P. Stilbs, A. Y. F. Cheung, A. M. Howe and A. R. Pitt, *Langmuir*, 2001, **17**, 7178.
53 P. C. Griffiths, A. Y. F. Cheung, R. Farley, A. Paul, R. K. Heenan, S. M. King, E. Pettersson, P. Stilbs and R. Ranganathan, *J. Phys. Chem. B*, 2004, **108**, 1351.
54 M. Rosen, *Surfactants and Interfacial Phenomena*, 3rd edn., Wiley and Sons, Chichester, England.
55 J. F. Rathman and J. F. Scamehorn, *J. Phys. Chem.*, 1984, **88**, 5807.
56 K. Meguro, H. Akusu and M. Veno, *J. Am. Chem. Soc.*, 1976, **53**, 145.
57 M. Meyer and L. Sepulvbeda, *J. Colloid Interface Sci.*, 1984, **99**, 536.
58 J. F. Rathman and J. F. Scamehorn, *Langmuir*, 1987, **3**, 372.
59 D. G. Hall and T. J. Price, *J. Chem. Soc., Faraday Trans.*, 1984, **80**, 1193.
60 H. Maeda, *J. Colloid Interface Sci.*, 2003, **258**, 390.
61 E. D. Goddard, *Interactions of surfactants with polymers and proteins*, 1993, CRC Press, Boca Raton, Fla.
62 P. C. Griffiths, P. Stilbs, A. M. Howe and T. Cosgrove, *Langmuir*, 1996, **12**, 2884.
63 E. Pettersson, D. Topgaard, P. Stilbs and O. Söderman, *Langmuir*, 2004, **20**, 1138.
64 J. B. Huang, M. Mao and B.-Y. Zhu, *Colloids Surf., A*, 1999, **155**, 339.
65 H. Gharibi, B. M. Razavizadeh and A. A. Rafati, *Colloids Surf., A*, 1998, **136**, 123.
66 S. Cinelli, G. Onori and A. Santucci, *Colloids Surf., A*, 1999, **160**, 3.
67 R. Zana, *Adv. Colloid Interface Sci.*, 1995, **57**, 1.
68 M. Manabe, A. Tokunaga, H. Kawamura, M. Shiomi and K. Hiramatsu, *Colloid Polym. Sci.*, 2002, **280**, 929.
69 P. C. Griffiths, N. Hirst, A. Paul, S. M. King, R. K. Heenan and R. Farley, *Langmuir*, 2004, **20**, 6904.
70 A. Paul and N. Hirst, Unpublished Results.
71 G. H. Lindquist and R. A. Stratton, *J. Colloid Interface Sci.*, 1976, **55**, 45.